Structures, Spectral and Electrochemical Properties of *N*-(Naphth-2-ylmethyl)-Appended Porphyrinogens

Jonathan P. Hill,*[a] Wolfgang Schmitt,[a] Amy Lea McCarty,[b] Katsuhiko Ariga,[c] and Francis D'Souza*[b]

Keywords: Porphyrinogen / Redox chemistry / Spectroelectrochemistry / Puckered macrocycles / Quinones

Alkylation of 5,10,15,20-tetrakis(3,5-di-*tert*-butyl-4-oxo-2,5-cyclohexadienylidene)porphyrinogen at its macrocyclic nitrogen atoms results in four multiply *N*-substituted products, which were isolated and characterized. The electrochemical and spectroelectrochemical properties of these compounds were determined. Molecular structures of the *N*-alkylated compounds are influenced strongly by intermolecular π-π stacking interaction between naphthyl groups leading to formation of dimers or stacked arrays of the macrocycle depending on multiplicity of substituents. The redox and spectral properties of the compounds are related to the increasing multiplicity of *N*-substitution.

Introduction

Tetrapyrroles are ubiquitous in nature and are also of interest to synthetic and coordination chemists.[1] Their characteristic photo- and redox chemistries have attracted much attention and a large body of data regarding these and other properties has been accumulated.[1,2] Porphyrin chemistry is a burgeoning area and can hardly be considered as only regarding tetrapyrroles because of the application of modern synthetic methods, which has resulted in many new types of related macrocycles. These include non-nitrogen heteromacrocycles,[3] larger cyclic oligopyrroles[4] and *N*-confused porphyrins.[5]

However, much of this recent chemistry has entailed either peripheral modification of the porphyrin skeleton or expansion of the oligopyrrole core and very little effort has been spent to modify at the nitrogen atoms (except by heteroatom replacement). This is because substitution at the porphyrin N atoms requires loss of some of the features that are considered to make the compounds porphyrinic, i.e. metal chelation, planarity or aromaticity. Examples of porphyrin *N*-alkylation were reported previously, but the compounds have not been as extensively studied as the other tetrapyrroles because of difficulties both with preparation and stability, and despite interesting structural and physical characteristics.[6–8] More recently, an example of *N*-alkylation of one of the higher oligopyrroles has appeared.[9] The structures and electrochemistry of those compounds illustrate the potential that lies in the introduction of *N*-substituents at the oligopyrrole core.

Porphyrinogens are much more accessible than porphyrins for chemistry involving the pyrrolic nitrogen atoms although this has been mostly restricted to their metal coordinating abilities and the chemistry of the resulting complexes.[10,11] There are several porphyrinogens known where the *meso* substituents maintain conjugation of the tetrapyrrole system so that their electronic structures vary substantially from the nonconjugated porphyrinogens. The most notable examples of these are the *meso*-oxo-OEP **1** and *meso*-methylene-OEP **2** (OEP = β-octaethylporphyrinogen) of Inhoffen[12] and Otto et al.,[13] respectively, and the *meso*-tetrakis(3,5-di-*tert*-butyl-4-oxo-2,5-cyclohexadienylidene)porphyrinogen (**3**) first reported by Milgrom[14] (Scheme 1). All of these compounds likely exist as highly puckered entities, and this was illustrated by a crystal structure determination for the latter.[15] *N*-Alkylation of **3** was later shown to be a useful way of stabilizing the structure of the compounds against protic tautomerism.[16] Crystal structure determinations reveal that *N*-alkylation of **3** occurs in a stepwise fashion and without altering the conformation of the pyrrolic rings.[17] This limits isomeric possibilities and allows use of this stable conjugated porphyrinogen scaffold for various purposes. In fact, many kinds of functional group can be introduced selectively at the nitrogen atoms by variation of the alkylating reagent and subsequent chemical modification of the substituent where appropriate.[16,18]

We considered that compound **3** is an excellent precursor for electrochemically active compounds, and we are exploiting this by preparation of several families of derivatives. Previously, the structures and electrochemistry of the *N*-benzylated derivatives were investigated and revealed

[a] International Center for Young Scientists, National Institute for Materials Science,
Namiki 1-1, Tsukuba, Ibaraki 305-0044, Japan
[b] Department of Chemistry, Wichita State University,
1845 N. Fairmount, Wichita, Kansas 67260-0051, USA
[c] Supermolecules Group, Advanced Materials Laboratory, National Institute for Materials Science,
Namiki 1-1, Tsukuba, Ibaraki 305-0044, Japan

 DOI: 10.1002/ejoc.200500257

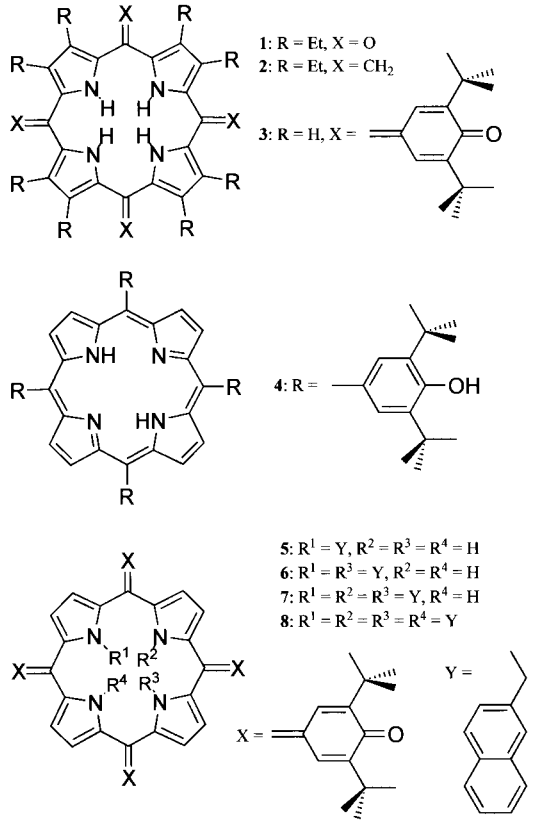

Scheme 1. Structures and abbreviations used for the investigated compounds.

stable anion and cation radicals as well as further species in higher and lower oxidation states.[17] On that occasion, only the high yield di- and tetra-*N*-alkylated compounds could be isolated. Subsequently, we have been able to isolate all of the available *N*-alkylates in the reaction between **3** and 2-(bromomethyl)naphthalene and we report here the results of structural, electrochemical and spectroelectrochemical analyses of these compounds.

Results

The compounds **5**–**8** were obtained in varying yields depending on reaction time. However, when a reactive alkyl halide such as a benzyl bromide is used in the *N*-alkylation of **3**, there is consistently a disparity in the yields of the variously substituted compounds so that the di- and tetra-*N*-substituted compounds are always obtained in moderate yield, while the mono- and tri-*N*-substituted derivatives are always of low yield. If a low-reactivity alkyl halide is used the rate of *N*-alkylation is slow enough that the mono-substituted derivative can be obtained in a reasonable yield although that of the tri-substituted derivative remains low. Apart from the reactivity of the alkyl halide, there are other factors that can affect the outcome of the reaction in terms of the yields of the variously substituted products. In these porphyrinogen molecules, there is the possibility of protic tautomerization where exchangeable hydrogen atoms can be located at central nitrogen or phenolic oxygen atoms. We believe that this is responsible for the unsymmetrical distribution of the products as, for instance, mono-*N*-alkylation forces the nitrogen opposing the initial alkylation site to be protonated thus increasing its reactivity towards an incoming alkyl halide. Such a situation is further complicated by the reaction solvent polarity, which can affect the distribution of tautomers of the starting porphyrinogen **3** and thus influence the relative yields of the products. Investigation of the factors affecting relative yields of *N*-alkylated derivatives of **3** is being undertaken in our laboratories.

X-ray Structural and Spectroscopic Characterization

The molecular structures of **6** and **8** determined by X-ray crystallography are shown in Figure 1. The orientations of *N*-substituents and conformations of the tetrapyrrole are similar to those already reported.[17,18] The most interesting feature of these crystal structures lies in the packing of the molecules, which is strongly influenced by a dipole–dipole interaction between the *N*-substituents. In fact, molecules of **6** contained within the structure are dimerized through this π-π stacking interaction, while the same effect operating in **8** gives a long-range ordering of the molecules into 1-dimensional arrays, which run parallel with the crystallographic *a*-axis. The π-π stackings in both **6** and **8** have intermolecular interplane distances of approx. 3.7 Å, which is similar to that observed in the solid-state structures of other polyaromatic molecules.[19] Previously, the π-π stacking effect has been used to introduce long-range order allowing observation of phenomena related to the close contact between aromatic systems,[20] and it can also be used to efficiently assemble discrete nanoscale objects.[21] Figure 1, parts A and C, show the molecular structure of **6** and its π-stacked dimeric unit. Figure 1, parts B and D, illustrate the molecular structure of **8** and how these molecules are forced to compose a 1D array through a similar π-stacking interaction. It is noteworthy that not all *N*-substituents are involved in stacking interactions. Thus in **6**, while one of the naphthyl groups is involved in intermolecular interactions, the other remains passive, ensuring formation of the dimeric unit. The same is true for **8** except that two naphthyl groups per molecule are passive in terms of the π-π stacking effect and a linear arrangement of the molecules results. The intermolecular stacking is mediated by the groups substituted on adjacent rather than opposing nitrogen atoms, i.e. N^{21} and N^{22}.

Figure 1E illustrates the binding of solvent molecules by hydrogen bonding to the free NH protons in **6**. The binding of water in this way is a general feature of the N^{21},N^{23}-disubstituted derivatives and allows capture of a secondary guest when that guest contains an alcohol group. The primary guest water molecule also apparently plays a role in fixing the conformation of the macrocycle.

Distortions of the tetrapyrrole framework can have important effects on the properties of these macrocycles. If we consider the dihedral angles between the least-squares mean

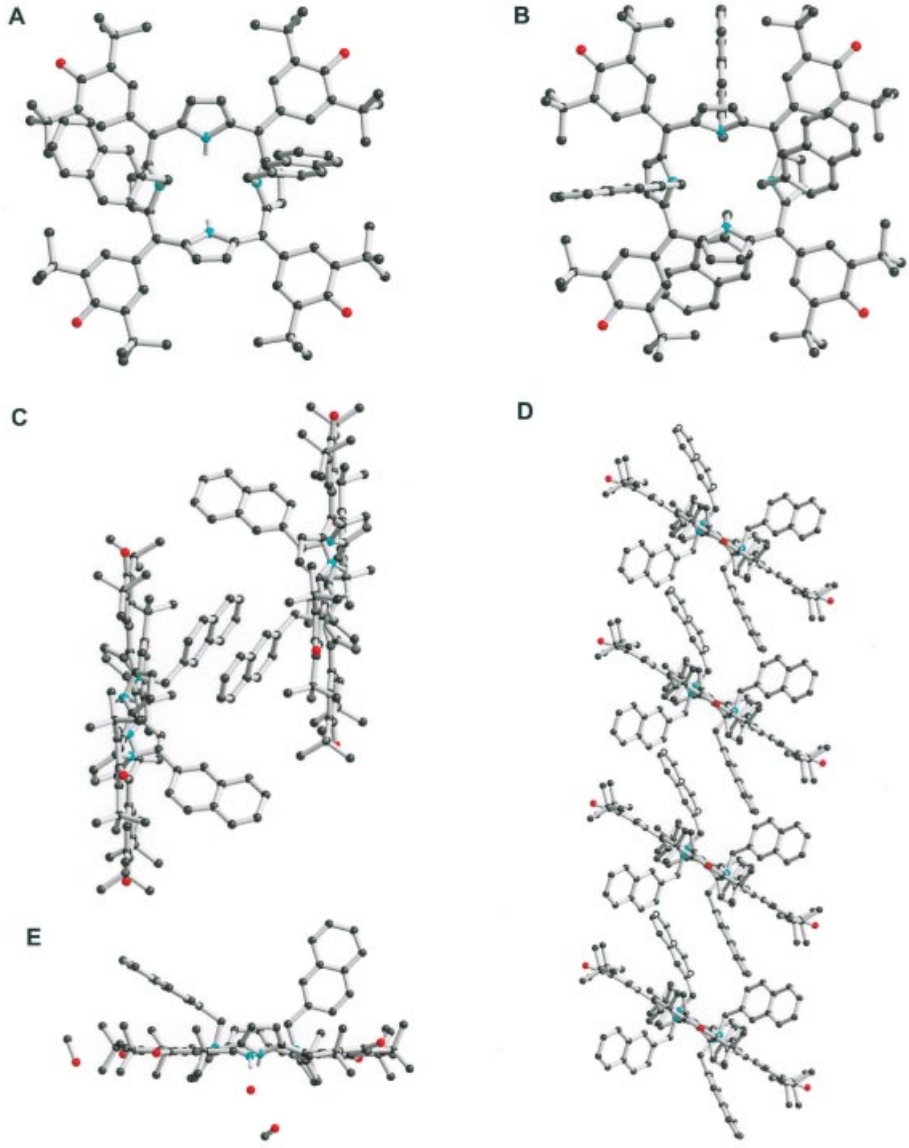

Figure 1. Molecular structure and packing arrangements in crystals of 5,10,15,20-tetrakis(3,5-di-*tert*-butyl-4-oxocyclohexa-2,5-dienylidene)-N^{21},N^{23}-bis(naphth-2-ylmethyl)porphyrinogen (**6**) and 5,10,15,20-tetrakis(3,5-di-*tert*-butyl-4-oxocyclohexa-2,5-dienylidene)-N^{21},N^{22},N^{23},N^{24}-tetrakis(naphth-2-ylmethyl)porphyrinogen (**8**). **A**. Structure of **6**. **B**. Structure of **8**. **C**. Dimeric species by stacking interactions in **6**. **D**. 1-Dimensional array of **8** formed by stacking interactions (runs parallel with crystallographic *a*-axis). **E**. Binding of water and secondary guest methanol through hydrogen bonding in **6**. (**A**–**D**. Hydrogen atoms and solvent molecules omitted for clarity.).

plane of the macrocycle and those of each pyrrole group some dependence of these angles on substituent identity and multiplicity emerges. In the case of **3**, all pyrrole groups are essentially equivalent with a dihedral angle of 48°. In the *N*-substituted derivatives, there is some deviation from this arrangement so that in **6** the respective dihedral angles for unsubstituted and *N*-substituted pyrroles are 45° and 56°. This represents a less puckered conformation than for the benzyl analogue where the angles 47°, 52.4° (NH pyrroles) and 60.8°, 68.0° (*N*-benzylpyrroles) were observed.[17] These changes in the dihedral angles are probably due to the presence of different packing arrangements within the crystals. However, they illustrate that there is still some degree of flexibility in the disubstituted species despite a substantial crowding at the macrocyclic core. For **8**, the average dihedral angle subtended between macrocyclic least-squares plane and pyrrole planes is 53°, which is the same as in the benzylic analogue.[17] Thus, the difference in packing between the naphth-2-ylmethyl derivative **8** and its benzyl analogue has little effect on the macrocyclic conformation and the small degree of flexibility available to the di-*N*-substituted compounds is effectively removed by complete *N*-alkylation.

Proton NMR spectroscopic data for the compounds **5**–**8** are a useful means for determination of structural perturbations that occur in solution. This is especially true for resonances due to amine and benzylic protons. The chemical shifts of these protons are related to the macrocyclic conformation and also reflect the increasing steric crowding at the nitrogen atoms. Figure 2 shows the NMR spectra of

compounds **5**–**8**. Amine protons are shifted to higher field with increasing substitution while the benzylic protons are shifted, on average, downfield. For the amine protons, the shift to higher field is caused by the reduction in conjugative overlap and an increased pyrrolic character of the component five-membered heterocycles. The downfield shift of the benzylic protons is probably related to their increasing proximity to the π-systems of the pyrrole rings as the number of *N*-substituents increases. In the case of **7**, an unsymmetry in the environment of the N^{21},N^{23}-substituent methylene protons is introduced by the presence of the *N*-substituent at the opposing face of the molecule at N^{22}, and the resonance due to those protons appears as a four peak system around δ = 4.7 ppm (denoted by an asterisk in Figure 2). This feature originates in the difference in shielding ability between the π-systems of an *N*-substituted pyrrole group (i.e. that of N^{22}) and that of an unsubstituted pyrrole group (i.e. that of N^{24}) so that the (N^{21}–CH_2 and N^{23}–CH_2) benzylic protons on opposing sides of the molecule are in different environments (Figure 2). In similarly tri-substituted derivatives containing smaller substituents,[18] no such splitting of the resonance due to these *N*-substituent methylene protons was observed indicating the severity of the restriction of rotation in the naphth-2-ylmethyl derivatives.

Importantly, trends in the chemical shift of the most structure sensitive protons in this system confirm that *N*-alkylation occurs without altering the conformation of the parent oxidized porphyrin. It is interesting to speculate whether the possibility of regioselective *N*-substitution also exists in the larger cyclo[*n*]oligopyrroles[9] since this feature dictates the utility of these highly puckered macrocycles as scaffolds for construction of more complex molecules.

The optical absorption spectra of the compounds investigated are shown in Figure 3. All of the porphyrinogen derivatives revealed strong spectral features covering the entire visible range. This is, in contrast to porphyrin **4**, which exhi-

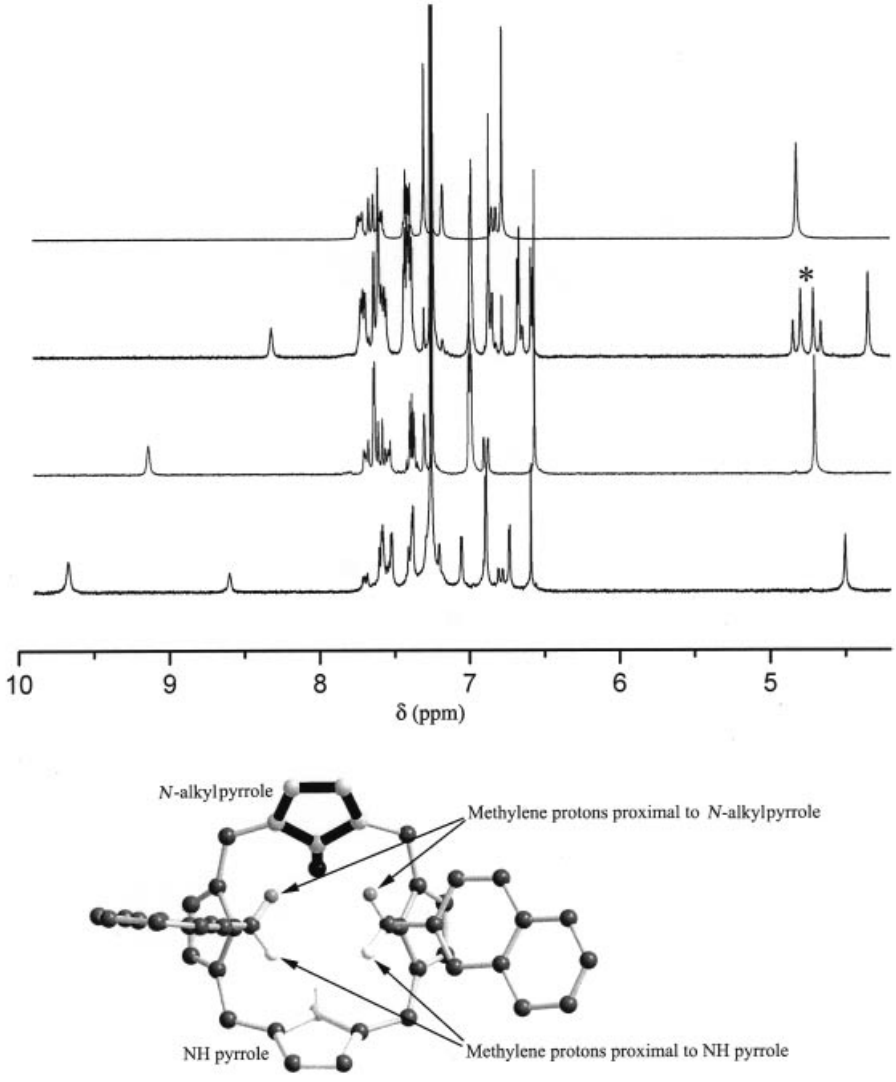

Figure 2. ^{1}H NMR spectra of **5**–**8** in the regions of aromatic and benzylic resonances. The structural model illustrates the difference in shielding environment of the methylene protons for the N^{21} and N^{23} alkyl groups in **7** and the asterisk denotes the resulting characteristic four line peak system.

Table 1. UV/Visible spectroscopic data (λ, nm) for the neutral, mono-anion and mono-cation species[a] of the *N*-(naphth-2-ylmethyl)-substituted tetrakis(oxocyclohexa-2,5-dienylidene)porphyrinogens in 1,2-dichlorobenzene.

Compound	Neutral	Neutral[b]	Mono cation	Mono anion
T(DtBHP)P, **4**[c]	**427**, 523, 561, 665	**429**, 524, 561, 567	429, 464, 560, 721	428, 464, 557, 729
Ox[T(DtBHP)P], **3**[c]	351, **518**, 598 (sh)	**534**, 598 (sh)	456, 598 (sh), 705	476, 552, 614 (sh), 769
Ox[T(DtBHP)P]Nh, **5**[c]	340, **513**, 579 (sh)	430, **525**, 594 (sh)	483, 525, 749	480, 564, 606, 745
Ox[T(DtBHP)P]Nh_2, **6**	344, **511**, 579 (sh)	443, **524,** 581 (sh)	523, 600 (sh), 752	531 (sh), 575, 739
Ox[T(DtBHP)P]Nh_3, **7**	333, **507**, 578 (sh)	445, **509,** 591 (sh)	425, 507, 603, 793	421, 507, 578 (sh), 742, 821
Ox[T(DtBHP)P]Nh_4, **8**	331, **505**, 568 (sh)	**505**, 568 (sh)	505, 717, 910	506, 722, 916

[a] The mono-anion and mono-cation were obtained by a spectroelectrochemical method. [b] In the presence of 0.1 M (TBA)ClO_4. [c] Irreversible spectral behaviour during oxidation and reduction.

bits an intense Soret band and weak visible bands typical of *meso*-substituted porphyrins. The peak position of the most intense Soret type band, as listed in Table 1 in bold, revealed a 2–5 nm blue shift upon successive addition of *N*-alkyl substituent at the porphyrinogen macrocycle.

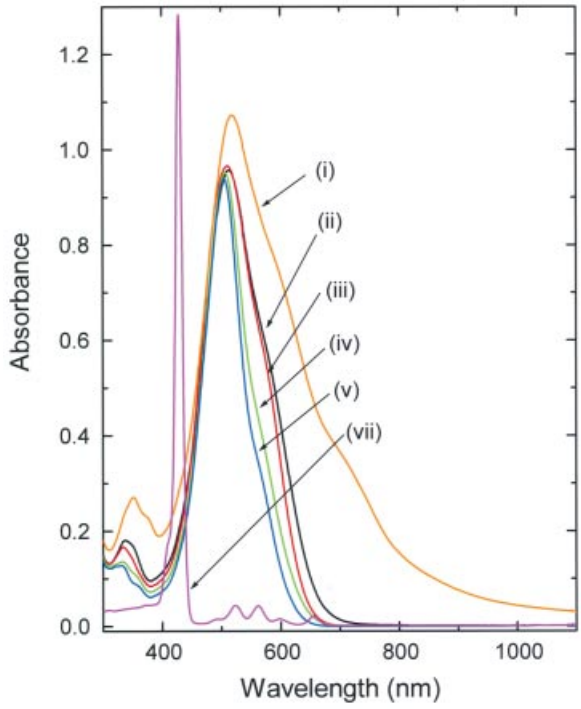

Figure 3. Optical absorption spectra of (i) tetrakis(3,5-di-*tert*-butyl-4-oxocyclohexa-2,5-dienylidene)porphyrinogen (**3**), (ii) 5,10,15,20-tetrakis(3,5-di-*tert*-butyl-4-oxocyclohexa-2,5-dienylidene)-N^{21}-(naphth-2-ylmethyl)porphyrinogen, (**5**), (iii) 5,10,15,20-tetrakis(3,5-di-*tert*-butyl-4-oxocyclohexa-2,5-dienylidene)-N^{21},N^{23}-bis(naphth-2-ylmethyl)porphyrinogen (**6**), (iv) 5,10,15,20-tetrakis(3,5-di-*tert*-butyl-4-oxocyclohexa-2,5-dienylidene)-N^{21},N^{23},N^{23}-tris(naphth-2-ylmethyl)porphyrinogen (**7**), (v) 5,10,15,20-tetrakis(3,5-di-*tert*-butyl-4-oxocyclohexa-2,5-dienylidene)-N^{21},N^{22},N^{23},N^{24}-tetrakis(naphth-2-ylmethyl)porphyrinogen (**8**) and (vi) *meso*-tetrakis(3,5-di-*tert*-butyl-4-hydroxyphenyl)porphyrin (**4**), in 1,2-dichlorobenzene.

Electrochemistry

Electrochemical studies, using the cyclic voltammetric technique, were performed to evaluate the redox potentials and to seek structure-reactivity relationships for the *N*-substituted porphyrinogens. In these studies dry, freshly distilled (CaH_2) 1,2-dichlorobenzene was used to prevent proton coupled chemical reactions that might occur upon electrochemical oxidation or reduction of the investigated compounds. Figure 4 shows the cyclic voltammograms of the porphyrinogens **3**, **5**, **6**, **7** and **8**, together with that of the porphyrin parent, *meso*-tetrakis(3,5-di-*tert*-butyl-4-hydroxyphenyl)porphyrin (**4**), while Table 2 lists the redox potentials for the electrochemical processes. The cyclic voltammogram of tetra-oxocyclohexadienylidene porphyrinogen **3**,

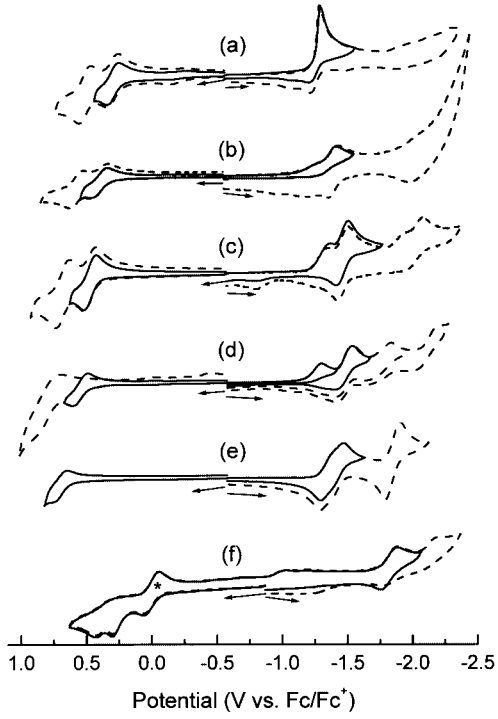

Figure 4. Cyclic voltammograms of (a) tetrakis(3,5-di-*tert*-butyl-4-oxocyclohexa-2,5-dienylidene)porphyrinogen (**3**), (b) 5,10,15,20-tetrakis(3,5-di-*tert*-butyl-4-oxocyclohexa-2,5-dienylidene)-N^{21}-(naphth-2-ylmethyl)porphyrinogen (**5**), (c) 5,10,15,20-tetrakis(3,5-di-*tert*-butyl-4-oxocyclohexa-2,5-dienylidene)-N^{21},N^{23}-bis(naphth-2-ylmethyl)porphyrinogen (**6**), (d) N^{21},N^{23},N^{23}-tris(naphth-2-ylmethyl)-5,10,15,20-(3,5-di-*tert*-butyl-4-oxocyclohexa-2,5-dienylidene)-porphyrinogen (**7**), (e) 5,10,15,20-tetrakis(3,5-di-*tert*-butyl-4-oxocyclohexa-2,5-dienylidene)-N^{21},N^{22},N^{23},N^{24}-tetrakis(naphth-2-ylmethyl)porphyrinogen (**8**) and (f) *meso*-tetrakis(3,5-di-*tert*-butyl-4-hydroxyphenyl)porphyrin (**4**), in 1,2-dichlorobenzene containing 0.1 M (TBA)ClO_4. Scan rate = 100 mV/s.

Table 2. Electrochemical redox potentials (V vs. Fc/Fc^+) of the *N*-(naphth-2-ylmethyl)-substituted tetrakis(oxocyclohexa-2,5-dienylidene)-porphyrinogens in 1,2-dichlorobenzene, 0.1 M $(TBA)ClO_4$. Scan rate = 100 mV/s.

Compound	2nd Ox	1st Ox	1st Red	2nd Red	3rd Red	4th Red
T(DtBHP)P, **4**	0.43[a]	0.31[a]	–1.82	–2.19	–	–
Ox[T(DtBHP)P], **3**	0.48	0.27	–1.33[b]	–	–	–
Ox[T(DtBHP)P]Nh, **5**	0.56	0.37	–1.29[b]	–1.44	–2.06[b]	–
$Ox[T(DtBHP)P]Nh_2$, **6**	0.69	0.47	–1.36[b]	–1.46	–1.95[b]	–2.04
$Ox[T(DtBHP)P]Nh_3$, **7**	0.81	0.54	–1.30[b]	–1.46	–1.75	–2.10
$Ox[T(DtBHP)P]Nh_4$, **8**	–	0.71	–1.32	–1.41	–1.85[c]	–1.85[c]

[a] E_{pa} at 0.1 V/s. [b] E_{pc} at 0.1 V/s. [c] Overlap of two one-electron processes.

bearing no *N*-substituents, contains two reversible oxidations located at $E_{1/2}$ = 0.27 and 0.48 V vs. Fc/Fc^+ and an irreversible reduction at E_{pc} = –1.33 V vs. Fc/Fc^+. The current required for the latter process is double that for the first oxidation suggesting a two-electron reduction process. Variable scan rate, multi-cyclic, and low-temperature (0 °C) voltammetric studies have little effect on the irreversibility of this reduction wave. Scanning the potential to –2.5 V revealed two more reductions at $E_{1/2}$ = –1.81 and –2.18 V, but these are not well defined. Compounds **5**–**8** bear an increasing number of naphth-2-ylmethyl entities at the macrocyclic nitrogen atoms and also exhibit reversible oxidation processes, while undergoing a systematic anodic shift in their oxidation potentials (Table 2).

Several interesting observations were made during the reduction of the *N*-substituted porphyrinogens. While the reduction of **4** is an irreversible two-electron process, the reductions of compounds **5**–**8** become increasingly reversible and the initial two-electron process is resolved into two reversible one-electron processes for the tetra-*N*-substituted compound, **8**. Scanning the potential further in the cathodic direction revealed up to two more one-electron reductions, which also become reversible with increase of the multiplicity of *N*-substituents on the macrocycle. For compound **8**, this wave involves two one-electron processes. The potential for the first reduction process is similar for all the derivatives. Conversely, the potentials of oxidation processes are anodically shifted by 70–130 mV for each additional *N*-substituent, indicating an increasing stabilization of the HOMO level upon *N*-substitution.[17] Previous ab initio calculations suggest a stabilized HOMO level for these *N*-substituted compounds.[17] As a result, the experimental HOMO–LUMO gap, calculated from the potential difference between the first oxidation and first reduction follow the trend: **3** < **5** < **6** < **7** < **8**, as predicted by the earlier computational studies for *N*-substituted porphyrinogens.[17]

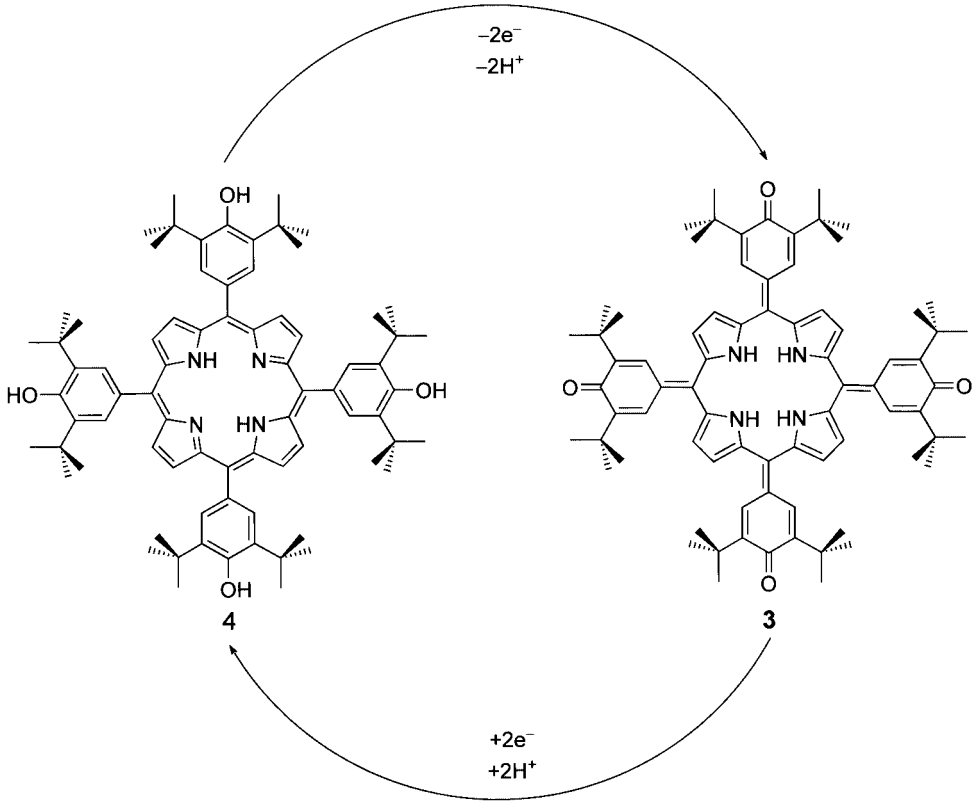

Scheme 2. Reversible interconversion between porphyrin and porphyrinogen involving two-electron/two-proton processes.

The initial two-electron reduction of compound **3** and the two one-electron reductions of compounds **5**–**8** can be rationalized based on Scheme 2. The transformation of *meso*-tetrakis(3,5-di-*tert*-butyl-4-hydroxyphenyl)porphyrins (**4**) to the tetrakis(oxocyclohexadienylidene)porphyrinogen **3** involves abstraction of two electrons and two protons. Similarly, one could envisage reversible conversion of **3** to **4** by the addition of two electrons and two protons. As a consequence, two facile and irreversible one-electron oxidations were observed for **4** (Figure 4, part f) while a facile, irreversible two-electron reduction process was observed for **3** (Figure 4, part a). The irreversible oxidation of **4** and irreversible reduction of **3**, even in dry solvent conditions, suggest conversion between them. The redox potentials also suggest that **4** is electron rich and that **3** is electron deficient. Assuming that the two-electron reduced product of **3** is doubly deprotonated **4**, one could argue that the potentials for the 3rd and 4th reductions should match that of compound **4**. Indeed, an examination of the voltammogram of **3** in the potential range of –1.5 to –2.3 V exhibits such reductions at potentials corresponding to the first and second reductions of **4**, although they are not fully developed. Substitution by *N*-substituents at the porphyrinogen nitrogen atoms not only increases the already puckered nonplanarity of the macrocycle as revealed by the X-ray and computational structures[17] but also causes resolution of the initial irreversible two-electron process into two reversible one-electron processes and improves the definition of the additional reductions.

Spectroelectrochemistry

In the presence of the supporting electrolyte 0.1 M (TBA)ClO_4, the absorption spectrum of the porphyrinogen **3** undergoes a 16 nm red shift of the most intense Soret-type band (see Table 1, values printed in bold). This shift in the band position decreased with increase of the number of *N*-substituents with virtually no shift for the tri- and tetra-*N*-substituted porphyrinogens. This shift suggests anion-binding of the supporting electrolyte to the porphyrinogen imino protons. This observation is similar to that found during anion binding by calix[4]pyrroles and other structurally related compounds.[22,23] A systematic study to elucidate the anion binding behavior of these porphyrinogens is being performed in our laboratories, and it will be discussed in detail elsewhere.

Assuming that the bound anion has no effect on the site of electron transfer of porphyrinogens, the spectroelectrochemical studies were performed in *o*-dichlorobenzene containing 0.1 M (TBA)ClO_4. Figure 5 presents the spectral changes observed during the oxidation and reduction of *N*-(naphth-2-ylmethyl) derivatives of **3** in *o*-dichlorobenzene containing 0.1 M (TBA)ClO_4, while the peak positions of the neutral, mono-cation and mono-anion species are listed in Table 1. The spectral changes recorded during the first oxidation of compounds **5**–**8** revealed a lowering of the intensity of the most intense peak located at ca. 500 nm with the appearance of new bands in the visible or near-IR region characteristic of the formation of the π-cation radical species. One or more isosbestic points were also observed indicating the presence of two species at equilibrium in solution. As expected, the spectral changes were also found to be reversible upon stepping the potential back to 0.0 V. The position of the new band corresponding to the formation of the π-cation radical depends upon the number of *N*-substituents on the porphyrinogen macrocycle. There is a systematic red shift of the newly developed low intensity absorption band. For compound **7** and **8**, this new absorption appears to be split into two bands located at 717 and 910 nm, respectively.

In accordance with the cyclic voltammetric observations, the spectral changes observed during the first reduction of compounds **3** and **5** are irreversible although new absorption peaks were observed during this process. For compounds **6**–**8**, the spectral changes are almost reversible and contain one or more isosbestic points. Since the first reduction is either overlapped or located close to the second reduction process for the compounds studied, a potential of 130 mV past the first/second reduction process was applied for spectroelectrochemical measurements. Under these conditions, two sets of spectral changes were observed, presumably corresponding to the one- and two-electron reduced products. The spectral changes shown in Figure 5 correspond to the initial spectral changes (i.e. first reduction). Under these conditions, the peak position of the emergent band, which corresponds to the formation of the porphyrinogen π-anion radical was found to depend on the number of *N*-substituents substituted at the porphyrinogen macrocycle, an observation similar to that observed for the π-cation radical species.

Discussion

We have extended our work on the *N*-alkylation of *meso*-tetrakis(3,5-di-*tert*-butyl-4-oxo-2,5-cyclohexadienylidene)porphyrinogen by the successful isolation and physical characterization of all the *N*-alkylates available from the direct reaction between **3** and 2-(bromomethyl)naphthalene in ethanol in the presence of potassium carbonate. Crucially, this has allowed complete electrochemical and spectroelectrochemical analysis of this interesting series of compounds. The structures of those compounds available by crystallography are influenced strongly by the π-π stacking interaction, where a dimeric or polymeric motif can be observed. In the case of the N^{21},N^{23}-disubstituted derivatives, potential host-guest systems are implicated by the capture of a water molecule and the coincidental binding of a secondary guest.

The observation of the well formed π-cation radical and π-anion radical spectra for the highly *N*-substituted porphyrinogens indicate their higher stability as predicted from the reversible redox processes and the spectral features extending into the near-IR region. Introduction of the *N*-substituents allows us greater access to discrete oxidized and

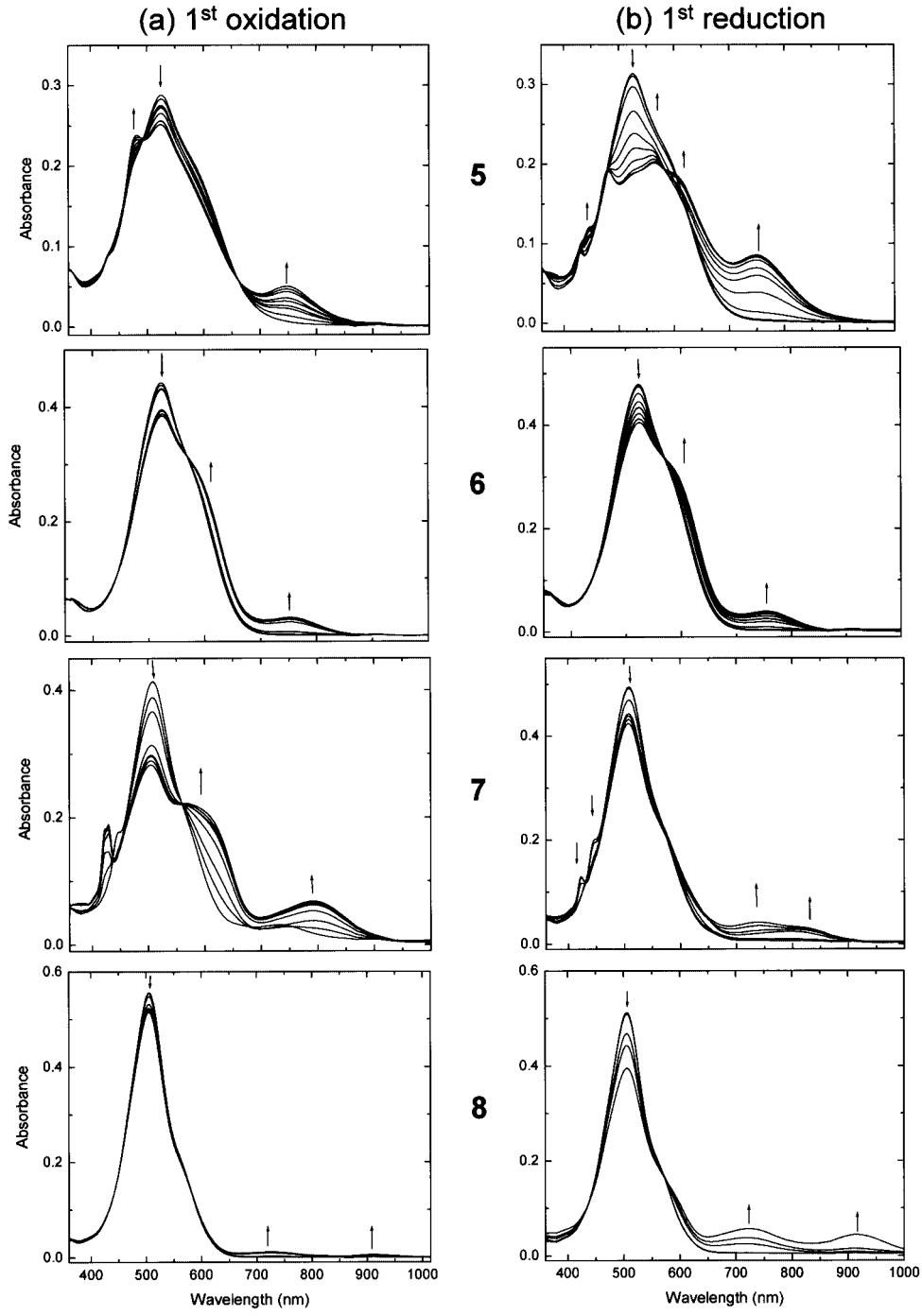

Figure 5. Spectral changes observed during (a) first oxidation and (b) first reduction of (i) 5,10,15,20-tetrakis(3,5-di-*tert*-butyl-4-oxocyclohexa-2,5-dienylidene)-N^{21}-2-(naphth-2-ylmethyl)porphyrinogen (**5**), (ii) 5,10,15,20-tetrakis(3,5-di-*tert*-butyl-4-oxocyclohexa-2,5-dienylidene)-N^{21},N^{23}-bis(naphth-2-ylmethyl)porphyrinogen (**6**), (iii) 5,10,15,20-tetrakis(3,5-di-*tert*-butyl-4-oxocyclohexa-2,5-dienylidene)-N^{21},N^{22},N^{23}-tris(naphth-2-ylmethyl)porphyrinogen (**7**), and (iv) 5,10,15,20-tetrakis(3,5-di-*tert*-butyl-4-oxocyclohexa-2,5-dienylidene)-N^{21},N^{22},N^{23},N^{24}-tetrakis(naphth-2-ylmethyl)porphyrinogen (**8**) in 1,2-dichlorobenzene containing 0.1 M (TBA)ClO_4.

reduced forms of the tetra(oxocyclohexadienylidene)porphyrinogen molecule. Additionally, variation of the multiplicity of substitution permits tuning of the redox properties of this system. Thus, when passing from **5** through **6** and **7** to **8**, not only are the reduced or oxidized states stabilized but there is a shift in the relative ease of oxidation and reduction processes so that increasing substitution results in higher oxidation potentials but lower reduction potentials. This is related to the enhanced stability of the intermediate oxidation states of the compounds upon substitution at the macrocyclic nitrogen atoms. The new absorption bands that appear at longer wavelength during redox processes add to the appeal of this system. The combination of oxidation state accessibility, redox potential "tunability"

and oxidation state-dependent absorption spectra is a useful tool in the design of multichromophoric and sensing systems. These features also imply potential applications in molecular memory devices or as electron transfer mediators in organic photovoltaic cells.

Currently, as well as investigation of the anion binding properties of the *N*-alkylated porphyrinogens, we are developing molecules which rely on the variable electrochemical and emissive properties of this and other similar systems. The introduction of more strongly interacting *N*-substituents is being investigated as a method for preparation of networked assemblies, and this oxidized porphyrin module has been incorporated into much more complex supramolecular systems. Finally, we are attempting to determine whether the variation of dihedral angles subtended between macrocyclic least-squares plane and its constituent pyrrole groups, observed for the di-*N*-substituted benzyl and naphth-2-ylmethyl derivatives, can be coupled to the electrochemical processes in these compounds, allowing construction of electromechanical molecular devices.

Experimental Section

Solvents and reagents were obtained from Aldrich Chemical Co., Wako Chemical Co., Tokyo Kasei Chemical Co. or Kanto Chemical Co. 2-(Bromomethyl)naphthalene was obtained from Aldrich Chemical Co. All commercially available reagents were used without further purification except 1,2-dichlorobenzene which was distilled from calcium hydride immediately prior to use. Compounds **3** and **4** were prepared by modifications of a literature method.[14] NMR spectra were measured from $CDCl_3$ solutions of the samples using a JEOL AL300BX spectrometer, with tetramethylsilane as an internal standard. FTIR spectra were obtained from films of the compounds deposited on a barium fluoride disc, using a Thermo-Nicolet 670SX FTIR Spectrophotometer. MALDI-TOF-MS spectra were measured using dithranol as matrix at Shimadzu Corp.

X-ray Crystallography: Crystals of **6** and **8** were grown by vapour diffusion of methanol or ethanol into chloroform solutions of the compounds. Structure solutions were by direct methods and refinement with SHELXTL.[24] X-ray crystallographic data for **6**, $C_{98}H_{108}N_4O_4{\cdot}0.5\,CHCl_3{\cdot}2\,CH_3OH{\cdot}4.5\,H_2O$, were collected at 200 K with a Bruker SMART APEX diffractometer using graphite-monochromated Mo-K_α radiation (λ = 0.71073 Å). **6:** $C_{100.5}H_{125}Cl_{1.5}N_4O_{10.5}$, M = 1593.09 g/mol, crystal size 0.5 × 0.2 × 0.05 mm^3, crystal appearance: Olive rectangular plate; space group P-1, a = 15.178(5) Å, b = 17.110(5) Å, c = 19.540(6) Å, α = 102.447(6)°, β = 96.300(7)°, γ = 91.518(6)°, V = 4918.52(11) Å^3, Z = 2, $\rho_{calcd.}$ = 1.076 mg/m^3, μ(Mo-K_α) = 0.541 mm^{-1}, 12842 reflections were measured ($2\theta < 45°$) of which 3959 were unique ($R_{int.}$ 0.1221). Refinement against F^2 to wR_2: 0.3203 (all data), R_1 [7118 reflections with $I > 2\sigma(I)$]: 0.1526, 1005 parameters, 0 restraints; all non-H atoms were anisotropic apart from those of the disordered solvent molecules. Data for compound **8**, $C_{120}H_{119}N_4O_4{\cdot}2\,CHCl_3{\cdot}0.5\,C_2H_5OH$, were collected at 200 K (Gemonochromated, λ = 0.8000 Å) at beamline PF-BL18B of the High Energy Accelerator Research Organization (KEK). X-ray data indicated no significant crystal decay during data collection. **8:** $C_{123}H_{126}Cl_6N_4O_{4.5}$, M = 1937.93 g/mol, crystal size 0.5 × 0.3 × 0.25 mm^3, crystal appearance: Red, rectangular plate; space group $P21/c$, a = 11.448(2) Å, b = 34.117(7) Å, c = 28.277(6) Å, β = 98.855(3)°, V = 10192.28(4) Å^3, Z = 4, $\rho_{calcd.}$ = 1.180 mg/m^3, 15675 reflections were measured ($2\theta < 51.2°$) of which 13592 were unique ($R_{int.}$ 0.0249). Refinement against F^2 to wR_2: 0.0798 (all data), R_1 [13592 reflections with $I > 2\sigma(I)$]: 0.0716, 1221 parameters, 0 restraints; all non-H atoms were anisotropic apart from those of the disordered solvent molecules.

CCDC-268484 (for **8**) and 268485 (for **6**) contain the supplementary crystallographic data for this paper. These data can be obtained free of charge from The Cambridge Crystallographic Data Centre via www.ccdc.cam.ac.uk/data_request/cif.

Electrochemistry and Spectroelectrochemistry: Cyclic voltammograms were recorded using a three-electrodes system. A platinum button electrode was used as the working electrode. A platinum wire served as the counter electrode and an Ag/AgCl electrode was used as the reference. Ferrocene/ferrocenium redox couple was used as an internal standard. All the solutions were purged prior to electrochemical and spectral measurements using argon gas. Spectroelectrochemical measurements were performed either on a Princeton Applied Research (PAR) diode array rapid scanning spectrometer or a Shimadzu UV/Visible spectrophotometer using a home-made cell with optically transparent (platinum mesh) electrodes. All the experiments were carried out at 23 ± 1 °C.

Preparation of Compounds 5–8: The compounds were prepared by a modification of a previously reported procedure[17,18] in which *meso*-tetrakis(3,5-di-*tert*-butyl-4-oxo-2,5-cyclohexadienylidene)porphyrinogen (100 mg, 9 × 10^{-5} mol) was *N*-alkylated by reaction with 2-(bromomethyl)naphthalene (3 equiv., 60 mg, 2.7 × 10^{-5} mol) in ethanol in the presence of anhydrous potassium carbonate (300 mg). Reaction progress was monitored by TLC and after consumption of the starting tetrapyrrole the reaction was quenched by pouring into water, and the mixture extracted with chloroform (2 × 50 mL). The extracts were dried (Na_2SO_4) then filtered, and the solvents were evaporated. The resulting green solid was chromatographed over silica gel eluting with dichloromethane. Four highly colored fractions were collected. The first and third fractions were identified as **8** and **6**, respectively, and were used for physical analyses without further purification. The second and fourth fractions were identified as **7** and **5**, respectively, but required further purification by column chromatography (SiO_2/CH_2Cl_2) before being subjected to physical analyses.

5,10,15,20-Tetrakis(3,5-di-*tert*-butyl-4-oxo-2,5-cyclohexadienylidene)-*N*-(naphth-2-ylmethyl)porphyrinogen (5): Yield: 6 mg (5%). FT-IR (BaF_2): $\tilde{\nu}$ = 3574.7 (NH, br, w), 3428.6 (NH, br, w), 3234.4 (NH, br, w), 2999.4 (w, CH), 2956.2 (m, CH), 2921.3 (m, CH), 2863.1 (w, CH), 1638.8 (w), 1596.5 (s), 1574.5 (sh), 1555.8 (sh), 1485.9 (m), 1459.4 (m), 1453.6 (m), 1419.0 (w), 1405.4 (w), 1388.1 (w), 1360 (s), 1334.0 (w), 1300.8 (m), 1261.6 (m), 1204.4 (w), 1176.7 (w), 1089.1 (m), 1028.3 (m), 996.8 (w), 942.3 (w), 930.0 (w), 886.9 (w), 837.9 (w), 819.4 (w), 800.1 (w), 755.7 (w). ^{1}H NMR (300 MHz, $CDCl_3$, 40 °C): δ = 1.12 [s, 18 H, –C(C*H*$_3$)], 1.32,1.33,1.35 [overlapping singlets, 56 H, –C(C*H*$_3$)], 4.47 (s, 2 H, *N*-benzylic *H*), 6.59 (s, 2 H, cyclohexadienyl-*H*), 6.75 (d, ^4J = 1.84 Hz, 2 H, cyclohexadienyl-*H*), 6.85 (d, ^3J = 8.81 Hz, 1 H, naphthyl-*H*), 6.88 (m, 4 H, cyclohexadienyl H, naphthyl-*H*), 7.06 (d, ^4J = 2.39 Hz, 2 H, cyclohexadienyl-*H*), 7.17 (s, 1 H), 7.38 (m, 4 H), 7.51–7.69 (m, 7 H), 8.49 (s, 1 H, N*H*), 9.28 (s, 2 H, N*H*) ppm. MS (MALDI, dithranol) ($C_{87}H_{102}N_4O_4$): 1266.57 ([M + 2H]$^+$).

5,10,15,20-Tetrakis(3,5-di-*tert*-butyl-4-oxo-2,5-cyclohexadienylidene)-*N*^{21},*N*^{23}-bis(naphth-2-ylmethyl)porphyrinogen (6): Yield: 44 mg (35%). FT-IR (BaF_2): $\tilde{\nu}$ = 3566.9 (br., w, NH), 3422.9 (br., w, NH), 3290 (br., w, NH), 3182.6 (br. w, NH), 2997.6 (w, CH), 2955.3 (m), 2915.5 (m), 2883 (sh, m), 2864.3 (m), 1632.6 (w), 1597.1

(s), 1563.6 (w), 1531.8 (w), 1488.6 (m), 1454.5 (m), 1404.9 (w), 1387.6 (w), 1360.9 (s), 1329.7 (m), 1310.4 (m), 1296.1 (m), 1261.1 (m), 1229.7 (w), 1205.5 (w), 1088.5 (m), 1028.7 (m), 948.6 (m), 926.8 (w), 886.3 (w), 855.6 (w), 840.7 (w), 817.0 (w), 805.5 (w), 772.3 (w), 755.9 (w). ^{1}H NMR (300 MHz, $CDCl_3$, 40 °C): δ = 1.09 [s, 36 H, –C(CH_3)], 1.35 [s, 36 H, –C(CH_3)], 4.71 (s, 4 H, benzylic-*H*), 6.57 (s, 4 H, cyclohexadienyl-*H*), 6.88–6.99 (dd, $^3J_1$ = 8.45, $^4J_2$ = 1.84 Hz, 2 H), 7.00 (m, 8 H, cyclohexadienyl H, naphthyl-*H*), 7.30 (s, 2 H), 7.35–7.42 (m, 4 H), 7.53–7.56 (m, 2 H), 7.59 (d, ^3J = 8.45 Hz, 2 H), 7.64 (d, ^3J = 2.57 Hz, 2 H, β-pyrrolic-*H*), 7.70 (m, 2 H), 9.14 (s, 2 H, N*H*) ppm. MS (MALDI, dithranol) ($C_{98}H_{109}N_4O_4$): 1406.59 ([M + H]$^+$).

5,10,15,20-Tetrakis(3,5-di-*tert*-butyl-4-oxo-2,5-cyclohexadienylidene)-*N*^{21},*N*^{22},*N*^{23}-tris(naphth-2-ylmethyl)porphyrinogen (7): Yield: 4 mg (3%). FT-IR (BaF_2): $\tilde{\nu}$ = 3444.0 (br., w, NH), 2998.2 (w), 2955.9 (m), 2919.7 (m), 2883.7 (w), 2864.7 (w), 1639.5 (w), 1596.6 (s), 1559.3 (w), 1527.1 (w), 1491.5 (m), 1455.0 (m), 1402.6 (w), 1387.7 (w), 1360.5 (s), 1330.4 (sh), 1303.7 (m), 1260.3 (w), 1220.9 (w), 1202.4 (w), 1088.8 (m), 1043.6 (m), 1024.93 (w), 947.2 (w), 929.5 (w), 918.5 (w), 888.4 (w), 805.8 (w), 772.3 (w), 755.2 (w). ^{1}H NMR (300 MHz, $CDCl_3$, 40 °C): δ = 1.09, [s, 18 H, –C(CH_3)], 1.12 [s, 18 H, –C(CH_3)], 1.23 [s, 18 H, –C(CH_3)], 1.35 [s, 18 H –C(CH_3)], 4.35 (s, 2 H, benzylic-*H*), 4.66–4.85 (two doublets, ^2J = 15.06 Hz, 4 H, benzylic-*H*), 6.58 (d, ^3J = 3.67 Hz, 2 H, cyclohexadienyl-H), 6.86 (m, 5 H), 6.99 (m, 4 H), 7.26 (s, 3 H), 7.38–7.44 (m, 8 H), 7.56–7.73 (m, 11 H), 8.32 (s, 1 H, N*H*) ppm. MS (MALDI, dithranol) ($C_{109}H_{117}N_4O_4$): 1546.64 ([M + H]$^+$).

5,10,15,20-Tetrakis(3,5-di-*tert*-butyl-4-oxo-2,5-cyclohexadienylidene)-*N*^{21},*N*^{22},*N*^{23},*N*^{24}-tetrakis(naphth-2-ylmethyl)porphyrinogen (8): Yield: 57 mg (38%). FT-IR (BaF_2): $\tilde{\nu}$ = 2998.1 (w), 2953.8 (m), 2920.3 (m), 2863.7 (m), 1639.9 (w), 1630.8 (w), 1598.4 (s), 1565.18 (w), 1525.1 (m), 1492.5 (m), 1455.0 (m), 1402.2 (w), 1387.5 (w), 1375.6 (w), 1360.3 (s), 1331.8 (w), 1316.5 (m), 1255.5 (m), 1223.4 (w), 1202.7 (w), 1175.8 (w), 1088.7 (m), 1047.7 (m), 1017.8 (w), 961.7 (w), 947.4 (w), 939.4 5 (w), 929.7 (w), 889.2 (w), 862.9 (w), 845.4 (w), 837.2 (w), 819.5 (w), 807.8 (m), 803.4 (m), 789.4 (w), 738.6 (m). ^{1}H NMR (300 MHz, $CDCl_3$, 40 °C): δ = 1.16 [s, 72 H, –C(CH_3)], 4.82 (s, 8 H, benzylic-*H*), 6.78 (s, 8 H, cyclohexadienyl-*H*), 6.82–6.85 (dd, 4 H), 7.18 (s, 4 H), 7.30 (s, 8 H, β-pyrrolic-*H*), 7.39–7.44 (m, 8 H), 7.58–7.61 (m, 4 H), 7.65 (d, 4 H), 7.71–7.75 (m, 4 H) ppm. MS (MALDI, dithranol) ($C_{120}H_{125}N_4O_4$): 1686.63 ([M + H]$^+$).

Acknowledgments

This work was supported by the Special Coordination Funds for Promoting Science and Technology from MEXT, Japan via ICYS Fellowships (J.P.H., W.S.), Petroleum Research Funds administered by the American Chemical Society and National Institutes of Health (to FD). This work has been performed under the approval of the Photon Factory Program Advisory Committee (Proposal No. 04G238).

[1] a) *The Porphyrins*; vols. 1–7 (Ed.: D. Dolphin), Academic Press: New York, **1978**; b) L. R. Milgrom, *The Colors of Life,* Oxford University Press, **1997**.
[2] *The Porphyrin Handbook* (Eds.: K. M. Kadish, K. M. Smith, R. Guilard), Academic Press: New York, **2000**.
[3] a) L. Latos-Grażyński, in *The Porphyrin Handbook* (Eds.: K. M. Kadish, K. M. Smith, R. Guilard), Academic Press, New York, **2000** vol. 2, p. 361; b) D. Liu, T. D. Lash, *Chem. Commun.* **2002**, 2426–2427; c) S. K. Pushpan, T. K. Chandrashekar, *Pure Appl. Chem.* **2002**, *74*, 2045–2055.
[4] a) J. L. Sessler, A. Gebauer, S. J. Weghorn, *Expanded Porphyrins*, in *The Porphyrin Handbook* (Eds.: K. M. Kadish, K. M. Smith, R. Guilard), Academic Press: Burlington, MA, **2000**; vol. 2, chapter 9; b) A. Jasat, D. Dolphin, *Chem. Rev.* **1997**, *97*, 2267–2340.
[5] a) H. Furuta, T. Asano, T. Ogawa, *J. Am. Chem. Soc.* **1994**, *116*, 767–768; b) P. J. Chmielewski, L. Latos-Grażyński, K. Rachlewicz, T. Głowiak, *Angew. Chem. Int. Ed. Engl.* **1994**, *33*, 779; *Angew. Chem.* **1994**, *106*, 805; c) G. R. Geier, D. M. Haynes, J. S. Lindsey, *Org. Lett.* **1999**; *1*, 1455–1458; d) J. P. Belair, C. J. Ziegler, C. S. Rajesh, D. A. Modarelli, *J. Phys. Chem. A* **2002**, *106*, 6445–6451.
[6] a) A. H. Jackson, in *The Porphyrins* (Ed.: D. Dolphin), Academic Press, New York, **1979**, vol. 1, 341; b) R. Grigg, A. Sweeney, G. R. Dearden, A. H. Jackson, A. W. Johnson, *Chem. Commun.* **1970**, 1273–1274.
[7] a) G. R. Dearden, A. H. Jackson, *Chem. Commun.* **1970**, 205–206; b) A. H. Jackson, R. K. Roberts, E. Pandey, *Chem. Commun.* **1985**, 470–471.
[8] D. K. Lavallee, *The Chemistry and Biochemistry of N-substituted Porphyrins*, VCH Publishers, New York, **1987**.
[9] T. Köhler, Z. Ou, J. T. Lee, D. Seidel, V. Lynch, K. M. Kadish, J. L. Sessler, *Angew. Chem. Int. Ed.* **2005**, *44*, 83–87.
[10] C. Floriani, R. Floriani-Moro, in *The Porphyrin Handbook* (Eds.: K. M. Kadish, K. M. Smith, R. Guilard), Academic Press: Burlington, MA, **2000**; vol. 3, chapters 24 and 25.
[11] a) C. Floriani, E. Solari, G. Solari, A. Chiesi-Villa, C. Rizzoli, *Angew. Chem. Int. Ed. Engl.* **1998**, *37*, 2245–2248; b) C. J. Woods, S. Camiolo, M. E. Light, S. J. Coles, M. B. Hursthouse, M. A. King, P. A. Gale, J. W. Essex, *J. Am. Chem. Soc.* **2002**, *124*, 8644–8652; c) J. L. Sessler, S. Camiolo, P. A. Gale, *Coord. Chem. Rev.* **2003**, *240*, 17–55.
[12] H. H. Inhoffen, J.-H. Fuhrhop, F. van der Haar, *Justus Liebigs Ann. Chem.* **1966**, *700*, 92–105.
[13] C. Otto, E. Breitmaier, *Liebigs Ann. Chem.* **1991**, 1347.
[14] L. R. Milgrom, *Tetrahedron* **1983**, *39*, 3895–3898.
[15] A. J. Golder, L. R. Milgrom, K. B. Nolan, D. C. Povey, *Chem. Commun.* **1989**, 1751–1753.
[16] L. R. Milgrom, J. P. Hill, G. Yahioglu, *J. Heterocyclic Chem.* **1995**, *32*, 97–101.
[17] J. P. Hill, I. J. Hewitt, C. E. Anson, A. K. Powell, A. L. McCarthy, P. A. Karr, M. E. Zandler, F. D′Souza, *J. Org. Chem.* **2004**, *69*, 5861–5869.
[18] E. Dolušić, S. Toppet, S. Smeets, L. V. Meervelt, B. Tinant, W. Dehaen, *Tetrahedron* **2003**, *59*, 395–400.
[19] P. T. Herwig, V. Enkelmann, O. Schmelz, K. Muellen, *Chem. Eur. J.* **2000**, *6*, 1834–1839 and references cited therein.
[20] A. M. van de Craats, J. M. Warman, K. Muellen, Y. Geerts, J. D. Brand, *Adv. Mater.* **1998**, *10*, 36–38.
[21] J. P. Hill, W. Jin, A. Kosaka, T. Fukushima, H. Ichihara, T. Shimomura, K. Ito, T. Hashizume, N. Ishii, T. Aida, *Science* **2004**, *304*, 1481–1483.
[22] P. A. Gale, J. A. Sessler, V. Kral, V. Lynch, *J. Am. Chem. Soc.* **1996**, *118*, 5140–5141.
[23] B. Dietrich, *Pure Appl. Chem.* **1993**, *65*, 1457–1464.
[24] G. M. Sheldrick, *SHELXTL 5.1*, Bruker AXS Inc., 6300 Enterprise Lane, Madison, WI 53719-1173, USA, **1997**.

Received: April 12, 2005
Published Online: June 9, 2005